Ore Geology Reviews 74 (2016) 39–51

Contents lists available at ScienceDirect

Ore Geology Reviews

journal homepage: www.elsevier.com/locate/oregeorev

Genesis and tectonic setting of ophiolitic chromitites from the Dehsheikh ultramafic complex (Kerman, southeastern Iran): Inferences from platinum-group elements and chromite compositions

Sima Peighambari [a,*], Ibrahim Uysal [b], Heinz-Günter Stosch [c], Hamid Ahmadipour [d], Hassan Heidarian [e]

[a] Department of Geology, Payame Noor University, P.O. Box 19395-3697, Tehran, Iran
[b] Karadeniz Technical University, Department of Geological Engineering, 61080 Trabzon, Turkey
[c] Karlsruhe Institute of Technology (KIT), Institute for Applied Geosciences, Kaiser Str. 12, 76131 Karlsruhe, Germany
[d] Department of Geology, Shahid Bahonar University of Kerman, P.O. Box 133-76135, Kerman, Iran
[e] Geoscience Faculty, Shahid Beheshti University of Tehran, Daneshju Blvd, P.O. Box: 1983963113, Tehran, Iran

ARTICLE INFO

Article history:
Received 21 May 2015
Received in revised form 30 October 2015
Accepted 31 October 2015
Available online 2 November 2015

Keywords:
Platinum-group elements
Chromite
Podiform chromitite
Ophiolite
Dehsheikh
Iran

ABSTRACT

Chromitite bodies of various sizes associated with dunite envelopes have been found in the Dehsheikh ultramafic massif, in the southeastern part of the outer Zagros ophiolite belt. The chromitites occur as layered and lenticular bodies, and show both magmatic and deformational textures, including massive, disseminated, banded and nodular types. The Dehsheikh chromitites display a variation in Cr# [100 × Cr / (Cr + Al)] from 69 to 78, which is typical of high-Cr chromitites. The Al_2O_3 and TiO_2 contents of chromites range from 10.3 wt.% to 16.9 wt.% and 0.12 wt.% to 0.35 wt.%, respectively. The Al_2O_3, TiO_2, and FeO/MgO values calculated for parental melts of Dehsheikh chromitites are within the range of boninitic melts. Chondrite-normalized distribution patterns of platinum-group elements show relative enrichments in Ru, Ir, and Os, and depletions in Rh, Pd, and Pt that are typical of chromitites associated with ophiolites formed by high degrees of mantle partial melting. The presence of Na-rich amphibole inclusions in chromite grains, together with the mineralogical and chemical composition of the chromitites and estimates of their parental melt compositions are used to help establish the tectono-magmatic setting. It is shown that the Dehsheikh massif is an ophiolite formed in a suprasubduction zone setting. We suggest that the composition of the rocks in this section was influenced by hydrous partial melts which might be formed in the subduction zone. Variable melt/rock interaction produced melt channel networks in the dunite which allowed the parental melt of the chromitite to percolate through them. Similar characteristics have been observed in other ophiolite complexes from the outer Zagros Iranian ophiolitic belt; these are believed to be the product of magmatism in a fore-arc environment.

1. Introduction

The origin of podiform chromitites and the nature of their geodynamic setting are still not completely understood. The composition of chromite minerals depends mostly on the degree of partial melting of the mantle sources and consequently reflects the parental magma (c.f. Rollinson, 2008) and also the geodynamic setting in which they formed (e.g., Cai et al., 2012; Dick and Bullen, 1984; Ghosh et al., 2013). Chromite chemical composition is often indicative of the source and bulk geochemistry of parental melts. For example, high Cr chromitites (Cr# > 0.60) may have crystallized from boninitic magmas, whereas high Al chromitites (Cr# < 0.60) may be derived from MORB-like tholeiitic magmas (Arai et al., 2011; Kamenetsky et al., 2001; Melcher et al., 1997; Zaccarini et al., 2011). The occurrence of podiform chromitites and their geochemical composition can be related to two main geodynamic settings, i.e., within supra-subduction zones and spreading centres in back-arc basins (e.g., Arai and Yurimoto, 1994, 1995; Nicolas, 1989; Roberts, 1988; Zhou and Robinson, 1997). Chromite can also be used as a petrogenetic indicator to help establish the composition of the primary mantle source.

The concentration and relative distribution of platinum-group elements (Ru, Rh, Pd, Os, Ir, and Pt) in mafic and ultramafic igneous rocks are controlled by processes such as partial melting, fractional crystallization, and degree of S-saturation of the magma. Depending on the melting temperature and geochemical affinity, the PGE have been divided into two sub-groups (Barnes et al., 1985): Ir-group elements (IPGE: Os, Ir, Ru) have high melting temperature (>2300 °C), whereas the Pd-group PGE (PPGE: Rh, Pt, Pd) are controlled by much lower melting temperatures (<2000 °C). Podiform chromitites are presently regarded

* Corresponding author at: Department of Geology, Payame Noor University, Tehran, Iran.
E-mail addresses: peighambari@pnu.ac.ir, peighambari.si@gmail.com (S. Peighambari).

http://dx.doi.org/10.1016/j.oregeorev.2015.10.032
0169-1368/

as sub-economic sources of the IPGE (Uysal et al., 2007a, 2007b). Ophiolite complexes with minor occurrences enriched in PPGE have been identified in the Shetland ophiolite in Scotland (Prichard et al., 1986; Brough et al., 2015), Acoje in the Zambales ophiolite in the Philippines (Bacuta et al., 1990), the Vourinos ophiolite (Greece; Konstantopoulou and Economou-Eliopoulos, 1991), Berit ophiolite (Turkey; Kozlu et al., 2014), and Al'Ays ophiolite (Saudi Arabia; Prichard and Brough, 2009; Prichard et al., 2008). The PGE abundance patterns record information about the genesis of ophiolitic chromitites and the peridotites that contain them (e.g., Akmaz et al., 2014; Garuti et al., 1997; Hamlyn et al., 1985; Naldrett, 1981; Uysal et al., 2009a, 2009b; Zhou et al., 1998).

In this paper, we present major element geochemical data and PGE concentrations for chromitites from the Dehsheikh ophiolitic massif to establish the nature of the chromitite parental melt and to infer both the tectonic setting and conditions of formation.

2. Geological background and field relationships

The Dehsheikh massif is one of the ultramafic massifs of the ophiolite belt in the southeastern Sanandaj–Sirjan zone and the main Zagros thrust belt (Fig. 1a). The Zagros fold thrust belt is part of the Bitlis–Zagros collision zone extending NW–SE from eastern Turkey through northern Iraq and the length of Iran to the Strait of Hormuz and into northern Oman; it was formed as an accretionary prism by a process of subduction of the Arabian plate beneath the Central Iranian plate (Shafaii Moghadam et al., 2010). The Upper Cretaceous Zagros ophiolites constitute the central parts of the Late Cretaceous Tethyan ophiolite belt, which extended for ~3000 km from Cyprus to Oman (Shafaii Moghadam et al., 2013). The Zagros ophiolites lie along the northeastern flank of the Zagros Fold Thrust Belt, which was formed during the late Cretaceous episode of subduction initiation on the northern side of the Neo-Tethys and show a fore-arc lithosphere (Fig. 1a) (Shafaii Moghadam et al., 2010). The Zagros ophiolites comprise two parallel belts; Fig: 1) an inner belt containing the Nain–Dehshir–Baft ophiolites, and 2) an outer belt consisting of the Kermanshah, Neyriz and Esfandagheh–Haji Abad ophiolites. The Esfandagheh–Haji Abad region is a tectonically active zone comprising several ultramafic–mafic complexes including the Soghan (Ahmadipour et al., 2003; Najafzadeh and Ahmadipour, 2014), Abdasht (Jannessary et al., 2012), Sikhoran (Ghasemi et al., 2002), and Dehsheikh (Peighambari et al., 2011) with combined chromite reserves of eight million tonnes at a grade between 30% and 53% Cr_2O_3). This region also contains the Sargaz–Abshur metamorphic complex including mica schist, amphibolites and greenschists (Sabzehei, 1974), a Jurassic–Cretaceous sedimentary–igneous association containing flysch, turbidites, and Calpionella limestone, and coloured mélange zones, such as Siahkuh and south Dowlatabad mélanges, granitoid bodies, and predominantly Palaeozoic to Tertiary Zagros sedimentary units.

McCall (1997) regarded the area in Fig. 3 as the southern margin of the Sanandaj–Sirjan–Bajgan–Durkan zone sliver separated from the Neyriz ophiolites. Shahabpour (2005) interpreted the ophiolite mélanges as a segment of the Neyriz ophiolite belt that is part of the southeastern edge of the main Zagros thrust belt. The Dehsheikh complex and other ultramafic–mafic complexes in the Esfandagheh–Haji Abad region have been interpreted as Alpine-type peridotites within

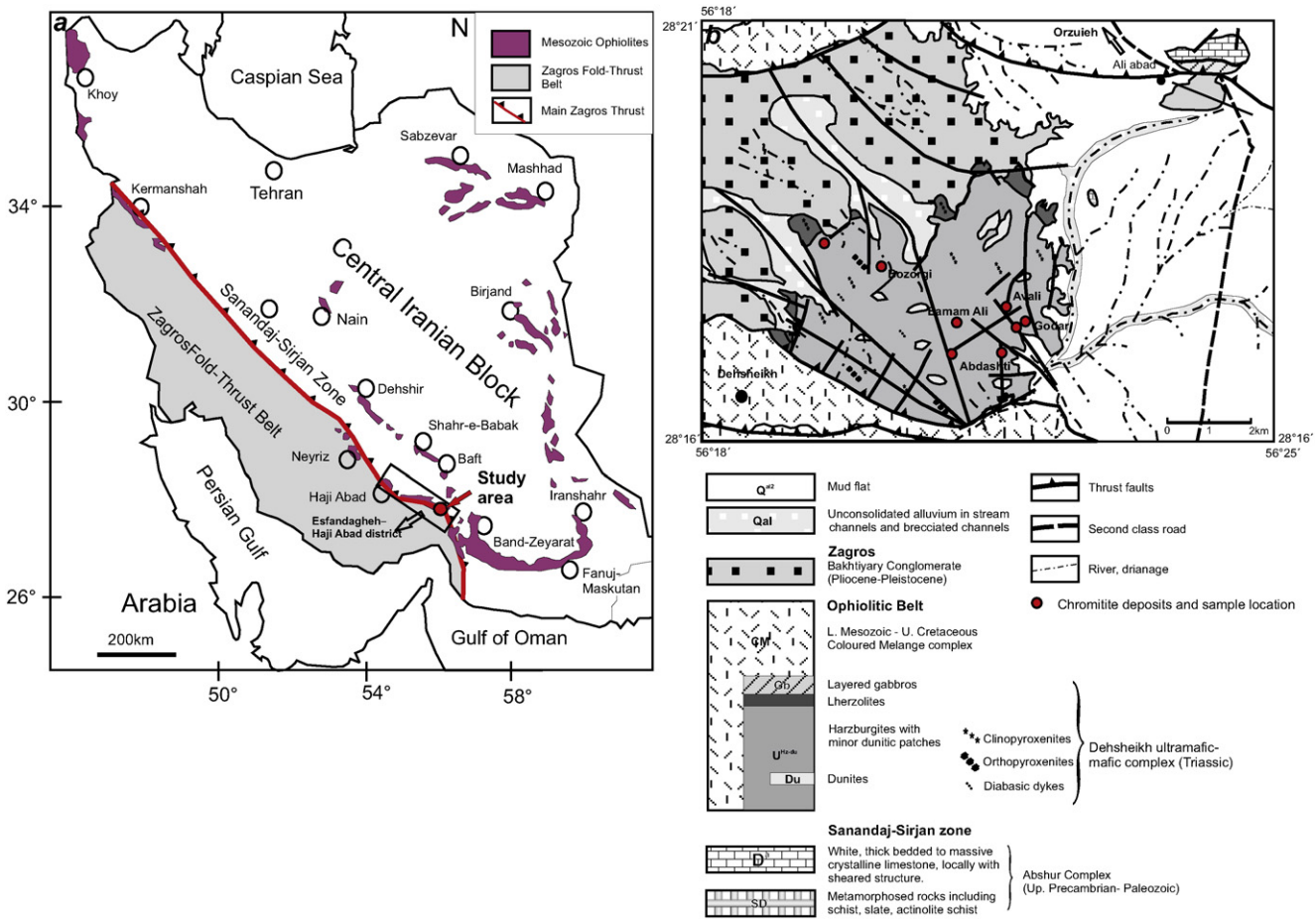

Fig. 1. a) Map showing the distribution of the Nain–Baft (inner) Zagros ophiolitic belt, the Kermanshah–Neyriz–HajiAbad (outer) Zagros ophiolitic belt, and the main Zagros thrust (MZT); b) Geological map of the Dehsheikh Massif with information on the position of chromite mines and sample localities.

an Upper Cretaceous ophiolite mélange within the Zagros thrust Zone (e.g., Ahmadipour et al., 2003; Jannessary et al., 2012; Najafzadeh and Ahmadipour, 2014; Shafaii Moghadam et al., 2010).

The Dehsheikh Complex mainly consists of harzburgite and dunite that contains chromitite deposits. Lherzolite occurs as small (up to 100 m) red to brown outcrops in the northern part of the massif. Two main dunite types are observed in the Dehsheikh complex. They form irregular patches that exhibit sharp contacts with harzburgites, and they occur as envelopes around chromitites that have been disrupted and separated from the ore bodies by plastic deformation. Chromitites and the associated dunite envelopes crop out in several locations in the Dehsheikh complex (Fig. 1b). The chromitite bodies have a lens or

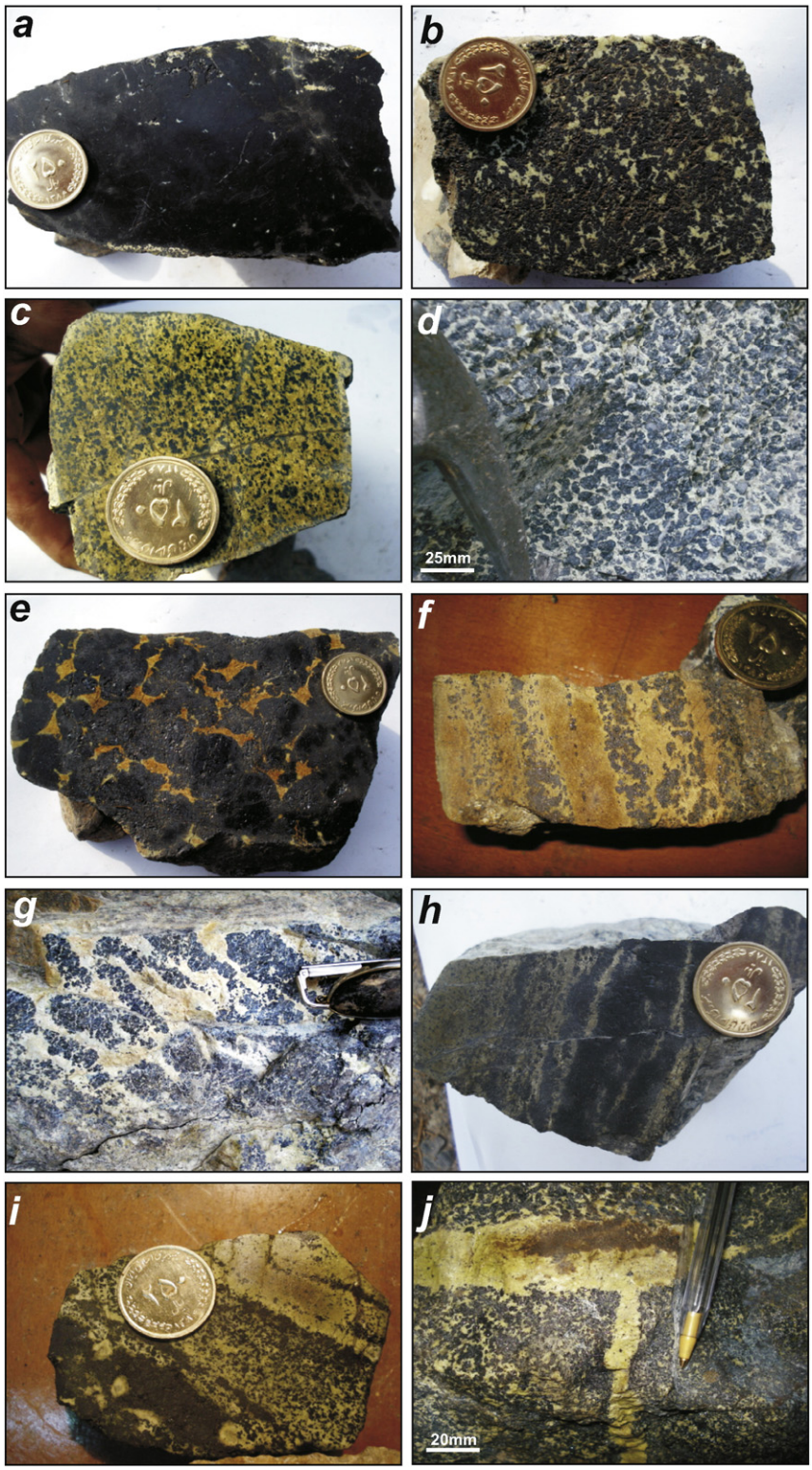

Fig. 2. Photographs of hand specimens of Dehsheikh chromitites, a) chromitite with massive texture and a high ratio of chromite/olivine, b) semi-massive chromitite texture; c) disseminated texture in Dehsheikh chromitites with low chromite/olivine ratio, d) and e) chromitites with nodular texture; f) chromitite with banded texture, g) and h) chromitite with folded and faulted texture, respectively, i) layered structure in chromitite, and j) dunite dyke in chromitites. The coin is 24 mm in diameter.

tabular morphology and they occur at the Emam Ali, Godar, Avali, Abdashti, and Bozorgi deposits that are located in the southeast and northwest of the Dehsheikh massif (Fig. 1b). Due to motion along faults, the primary igneous relationship between chromitites and their dunite envelope is unclear.

Different types of chromitite are observed including massive, semi-massive, disseminated, nodular, layered, occluded and brecciated, and also chromitites with deformed textures. Massive and semi-massive chromitites are fractured and composed of medium to coarse aggregates of chromite (Fig. 2a, b) consisting of subhedral to anhedral chromite grains (1–5 mm in diameter), whereas disseminated chromitites contain more euhedral fine- to medium-grained chromites (Fig. 2c). Nodular ores are observed in some mines (Fig. 2d, e). The nodules, which are entrained in a serpentinized matrix, have sizes between 0.5 cm and 3.0 cm, and consist of massive anhedral chromite grains. Banded chromitites (Fig. 2f) are composed of massive to disseminated subhedral to euhedral chromite grains in a serpentinized olivine matrix, and contain fine- to medium-grained chromite. Folded and faulted structures (Fig. 2g, h) are also found in phases of banded chromitites. Also, layering is sometimes observed in Dehsheikh chromitites where layers may have different textures, such as massive, disseminated, and nodular (Fig. 2i). Moreover, dunite dykes or bands are present in some chromitite samples with different textures (Fig. 2j).

3. Petrography

Harzburgite is the dominant ultramafic rock type in the Dehsheikh complex. Lherzolite and dunite are also present as small occurrences. Harzburgite shows protogranular to porphyroclastic textures, and contains 66–88 vol.% olivine, 15–27 vol.% orthopyroxene, 1–5 vol.% clinopyroxene, and 1–4 vol.% spinel. Harzburgite and other ultramafic rocks are relatively fresh and most primary silicate minerals display deformation features such as kinking and undulatory extinction. Sulphide phases occur as scattered grains in lherzolites (up to 1%) and rarely in harzburgites (up to 0.5%). Serpentinized dunite commonly envelops the podiform chromitite with sharp to gradual contacts. The transitions from dunite envelopes to harzburgitic country rocks are mostly sharp. Locally, pyroxenitic veins cut chromitites and their dunite envelope as well as their host harzburgites.

Under the microscope, the chromitites of Dehsheikh display magmatic textures; some chromitites are deformed. Massive chromitites consist of coarse subhedral–anhedral to subrounded interlocking chromite grains showing orthocumulate textures (Fig. 3a). Individual chromite grains show cumulate textures with very narrow interstices filled with serpentine (Fig. 3b). Brecciation and pull-apart textures (Fig. 3c, d) have been observed in some massive chromitites. Disseminated chromitites are composed of subhedral and subrounded chromite crystals (Fig. 3e) embedded in a matrix of silicate minerals such as olivine, serpentinized olivine, and clinopyroxene. In this type, chromite grains sometimes have inclusions of silicate minerals; in chromitites with nodular and banded structures, similar textures have been observed.

Chromites are usually fresh, showing typical ferrian-chromite alteration only along some grain boundaries and cracks (Fig. 3f). Olivine is the most abundant silicate mineral in the chromitites, and occurs both as a matrix mineral and inclusions. Other silicate phases, such as clinopyroxene and amphibole, occur between orthocumulate chromite grains. Serpentine group minerals typically replace olivine in the matrix and inclusions in chromite grains.

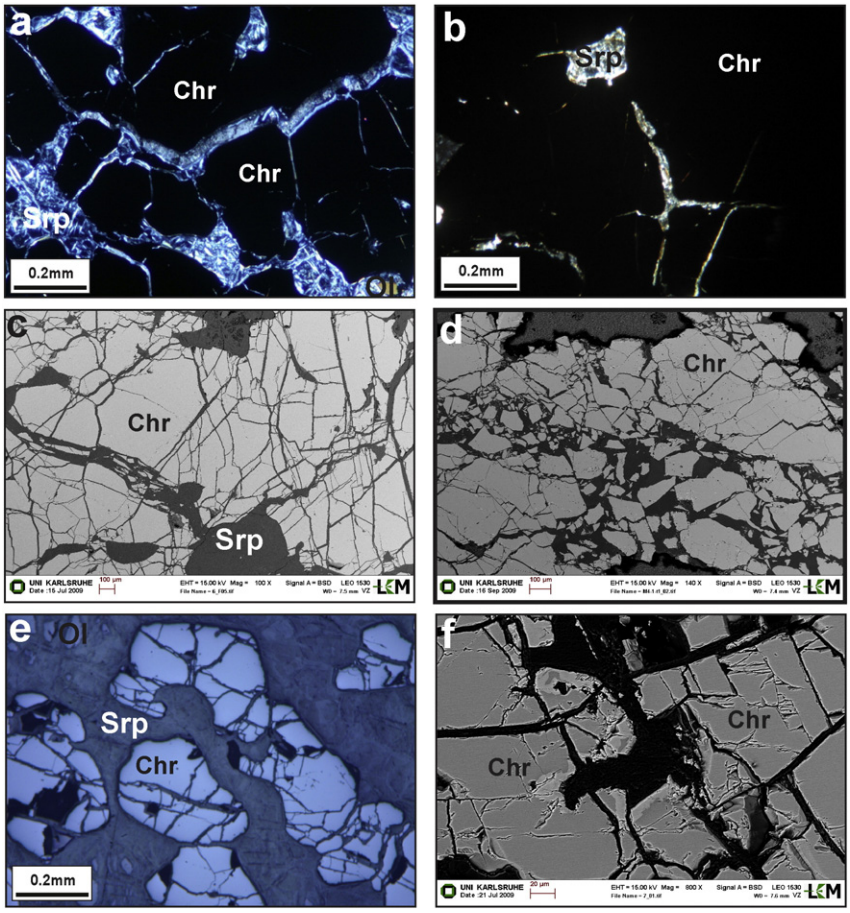

Fig. 3. Photomicrographs showing features of the Dehsheikh chromitites; a) orthocumulate texture in chromitites; b) cumulate texture; c) and d) pull-apart and brecciated texture in Dehsheikh chromitites; e) anhedral chromite grains in disseminated chromitites; f) ferrian-chromite alteration along some grain boundaries and cracks. Symbols are Chr as chromite grains, Ser as serpentine minerals, and Ol as olivine.

4. Analytical methods

Major elements of minerals were analysed in situ on polished thin sections using a JEOLJXA-8900 Superprobe at Münster University in Germany, operated at 15 kV accelerating potential with a 15 nA beam current using synthetic and natural standards. Spinel compositions were recalculated assuming stoichiometry to obtain Fe^{2+}/Fe^{3+}. The scanning electron microprobe (SEM) investigations were carried out at KIT (Karlsruhe). A total of 10 chromitite samples from different Dehsheikh chromitite pods were analysed for their PGE concentrations, using a nickel sulphide fire-assay pre-concentration method followed by ICP-MS analysis at Genalysis Laboratory, Perth, Western Australia. Detection limits were 1 ppb for Os, Ir, Ru, Pt, Pd, and Rh and 2 ppb for Au.

5. Mineral compositions

5.1. Chromite

Representative compositions of chromite from Dehsheikh chromitites are presented in Table 1. Sample 3 is from the dunite envelope. The

Table 1
Representative chromite compositions (wt.%) of chromitites from the Dehsheikh complex.

Sample	M4-1	M4-1	M4-1	M2-3	3*	4	5	6	F5	F5	M3-2	M3-2	M3-2	M3-2
Texture	Nod			Diss	Diss to Massive				Diss		Mass			
Chr/Ol	80%			60%	10%	60%	80%	90%	50%		80%			
Mine	Abdashti			Emam Ali	Bozorgi				Avali		Emam Ali			
SiO_2	0.04	0.01	0.01	0.03	0.01	0	0.02	0	0.05	0	0.02	0.01	0.01	0.02
TiO_2	0.24	0.12	0.19	0.18	0.32	0.24	0.28	0.29	0.18	0.228	0.26	0.24	0.23	0.26
Al_2O_3	13.98	12.92	12.93	13.83	19.6	16.9	15.81	16.18	12.52	13.19	13.44	13.57	13.40	13.44
Cr_2O_3	58.18	57.39	57.62	55.94	47.34	53.07	53.68	54.27	55.43	54.65	54.16	54.39	54.84	54.16
FeO	14.80	14.92	13.50	17.20	21.03	16.84	16.24	16.10	20.93	20.89	21.07	20.98	20.10	21.07
MnO	0.29	0.28	0.24	0.28	0.35	0.28	0.25	0.29	0.38	0.39	0.38	0.35	0.35	0.38
MgO	12.33	14.58	14.87	13.03	11.69	13.87	14.13	13.76	11.13	11.38	11.86	11.79	12.57	11.86
NiO	0.07	0.23	0.16	0.17	0.14	0.12	0.04	0.1	0.04	0.06	0.07	0.11	0.00	0.07
Total	99.93	100.45	100.37	100.5	100.3	101.2	100.3	100.9	100.6	100.72	101.26	101.33	101.50	101.18
Cations (structural formula on the basis of 4 oxygens)														
Ti	0.01	0.00	0.00	0.00	0.01	0.01	0.01	0.01	0.00	0.01	0.01	0.01	0.01	0.01
Al	0.53	0.48	0.48	0.52	0.72	0.62	0.58	0.59	0.48	0.50	0.51	0.51	0.50	0.51
Cr	1.47	1.43	1.44	1.40	1.17	1.30	1.33	1.34	1.42	1.39	1.37	1.37	1.37	1.37
Fe^{3+}	0.00	0.08	0.07	0.07	0.09	0.07	0.07	0.05	0.10	0.10	0.12	0.11	0.12	0.12
Fe^{2+}	0.40	0.31	0.30	0.38	0.45	0.36	0.34	0.36	0.46	0.45	0.43	0.44	0.40	0.43
Mn	0.01	0.01	0.01	0.01	0.01	0.01	0.01	0.01	0.01	0.01	0.01	0.01	0.01	0.01
Mg	0.59	0.69	0.70	0.62	0.55	0.64	0.66	0.64	0.54	0.55	0.56	0.56	0.59	0.56
Ni	0.00	0.01	0.00	0.00	0.00	0.00	0.00	0.00	0.00	0.00	0.00	0.00	0.00	0.00
Cr#[a]	73.63	74.87	74.93	73.07	61.84	67.81	69.49	69.23	74.81	73.54	73.00	72.89	73.30	73.00
Mg#[b]	59.76	69.01	69.97	61.82	54.67	64.18	65.9	63.99	53.85	54.81	56.56	56.14	59.53	56.56
(FeO/MgO)-melt[c]	0.99	0.63	0.60	0.89	1.33	0.85	0.77	0.85	1.2	1.16	1.08	1.11	0.96	1.08
TiO_2-melt[d]	0.35	0.21	0.29	0.61	0.44	0.36	0.40	0.42	0.28	0.34	0.35	0.35	0.34	0.38
Al_2O_3-melt[e]	12.71	12.30	12.30	12.65	14.47	13.70	13.35	13.47	12.13	12.40	12.50	12.55	12.49	12.50

M4t1	M4t1	M4t1	M1-3	M3-2	M1-2	M1-2	M1-2	M5-3	M5-3	M5-1	M5-1
Mass			Band	Nod	Band			Nod		Nod	Diss
90%			50%	70%	50%			60%		60%	50%
Abdashti			Avali	Emam Ali	Avali			Godar			
0.06	0.02	0.00	0.05	0.02	0.04	0.02	0.00	0.05	0.00	0.04	0.02
0.17	0.21	0.24	0.24	0.19	0.2	0.31	0.265	0.26	0.17	0.27	0.21
12.03	13.22	13.97	13.61	13.79	11.91	13.31	13.24	13.05	13.41	14.80	10.29
57.33	56.27	56.08	55.09	56.29	55.6	55.87	56.35	54.23	54.50	55.00	59.45
16.38	16.23	16.12	17.98	15.38	22.14	17.20	16.96	22.72	19.60	15.72	16.66
0.27	0.31	0.206	0.31	0.22	0.4	0.34	0.28	0.40	0.31	0.24	0.33
13.7	14.78	14.29	13.72	15.77	9.86	13.28	13.38	11.09	12.38	14.67	12.86
0.03	0.29	0.145	0.09	0.21	0.04	0.11	0.218	0.15	0.17	0.27	0.17
99.95	101.05	100.91	101.01	101.66	100.1	100.34	100.47	101.79	100.36	100.70	99.81
0.00	0.01	0.01	0.01	0.00	0	0.01	0.01	0.01	0.00	0.01	0.01
0.45	0.49	0.52	0.51	0.50	0.46	0.50	0.50	0.49	0.51	0.54	0.39
1.45	1.39	1.39	1.37	1.38	1.44	1.41	1.42	1.37	1.38	1.36	1.53
0.08	0.11	0.08	0.11	0.11	0.09	0.08	0.08	0.12	0.11	0.08	0.07
0.35	0.31	0.33	0.35	0.27	0.51	0.37	0.37	0.47	0.41	0.32	0.37
0.01	0.01	0.01	0.01	0.01	0.01	0.01	0.01	0.01	0.01	0.01	0.01
0.65	0.69	0.67	0.64	0.73	0.48	0.63	0.63	0.53	0.59	0.68	0.62
0.00	0.01	0.00	0.00	0.01	0.00	0.00	0.01	0.00	0.00	0.01	0.00
76.17	74.06	72.92	73.09	73.25	75.8	73.79	74.06	73.60	73.16	71.37	79.49
65.43	69.23	66.79	64.52	72.71	48.46	63.03	63.42	52.95	59.31	68.19	62.41
34.57	30.77	33.21	35.48	27.29	51.54	36.97	36.58	47.05	40.69	31.81	37.59
0.73	0.62	0.71	0.78	0.53	1.48	0.83	0.82	1.24	0.97	0.68	0.81
0.27	0.32	0.36	0.35	0.29	0.30	0.43	0.38	0.38	0,26	0.38	0.31
11.92	12.42	12.70	12.57	12.64	11.87	12.45	12.42	12.35	12.49	13.01	11.11

Diss: disseminated, Mass: massive, Nod: nodular, Band: banded.
[a]Cr#: 100 × Cr/(Cr + Al) atomic ratio.[b]Mg#: 100 × Mg/(Mg + Fe^{2+}) atomic ratio. [c]Augé (1987).[d and e]Rollinson (2008).
*From dunitic envelope.

compositions of chromites were obtained from the dunite envelope toward disseminated and massive chromitites (e in Fig. 4). Chromites from the dunite envelope have lower Cr_2O_3 and MgO contents than those from disseminated to massive chromitites, ranging from 45.45 to 48.78 wt.% and from 10.44 to 13.72 wt.%, respectively. The Al_2O_3 content is higher than those in chromitites, varying between 18.42 and 19.79 wt.%.

The Cr_2O_3 contents of chromites from disseminated to massive chromitites vary from 53.07 to 59.45 wt.% (averaging 55.26 wt.%) and Al_2O_3 contents from 10.29 to 16.9 wt.% (averaging 13.84 wt.%). The MgO and FeO contents vary from 9.8 to 15.45 wt.% (averaging 13.18 wt.%) and 14.35 to 22.72 wt.% (averaging 17.97 wt.%), respectively. Fig. 4e shows the variations of chromite composition from dunite envelope to massive chromitites. The corresponding Cr# varies from 62 to 70. Chromites from chromitites with nodular textures have the highest Cr#. The TiO_2 contents are low with a maximum content of 0.27 wt.%, which is typical of ophiolitic chromitites (Dick and Bullen, 1984; Arai, 1992; Ahmed, 2013). They also contain minor amounts of NiO (<0.29 wt.%).

The compositional data indicate that chromites from Dehsheikh chromitites are magnesiochromite and plot close to the boninite field in the Cr# vs. Mg# diagram shown in Fig. 5a. In the TiO_2 vs. Cr_2O_3 diagram, most chromite data fall into the podiform chromitites region, close to the boundary with the stratiform chromitites (Fig. 5b). Chromite grains from the dunite pods plot in the stratiform field (sample 2). A rough negative correlation between Al_2O_3 and Cr_2O_3 (Fig. 5c) in the Dehsheikh chromitites is also representative of their ophiolitic nature.

5.2. Olivine

Olivine compositions from Dehsheikh chromitite are given in Table 2. Olivine is the most common silicate mineral in Dehsheikh podiform chromitites, occurring as granular olivine in the dunite envelope and also as matrix and inclusions in chromite grains. In the dunite envelope the Fo [$100 \times Mg / (Mg + Fe^{2+})$] contents of olivine range from 92.3 to 92.9, and the NiO contents vary between 0.52 and 0.62 wt.%, whereas olivine in chromitite has higher Fo contents between 95 and 96, and NiO contents between 0.65 and 0.93 wt.%. Olivines from Dehsheikh chromitites have MnO contents ranging from 0.27 to 0.40 wt.%. In general, the olivines become more magnesian from the dunite envelope to the disseminated chromitite and massive chromitite (Fig. 4f). The NiO contents show an increase with increasing Fo values, whereas MnO contents appear to decrease with increasing Fo contents (Fig. 6a,b).

5.3. Other silicate minerals

Pyroxenes identified as inclusions inside chromite grains in chromitites are diopside ($En_{49.5}Fs_{1.2}Wo_{49.3}$) in composition, and have 0.86 to 0.93 wt.% Cr_2O_3 with negligible amounts of TiO_2 (<0.02 wt.%). Their Al_2O_3 contents vary from 0.80 to 1.00 wt.% and Na_2O contents reach a maximum of 0.49 wt.%. The electron microprobe data for amphibole inclusions in chromite display relatively high Na_2O contents ranging from 2.52 to 3.31 wt.% and Mg# of about 94, showing hornblende to edenite composition.

6. Platinum group element (PGE) geochemistry

The total PGE concentrations of Dehsheikh chromitite samples (Table 3) are typical of ophiolitic chromitites and vary from 60 to 300 ppb. Chromitites with massive textures show higher IPGE contents. All samples display relative enrichments in Ru (45–161 ppb), Ir (11–69 ppb) and Os (8–79 ppb) while their Rh and Pd contents range from 4 to 13 ppb and 2 to 5 ppb, respectively. Platinum is below the detection limit, except for samples M3, M4, M5-1 and 9, which contain 1 to 5 ppb Pt. All chromitite samples show negative slopes from Ru to Pd on the chondrite-normalized PGE diagram (Fig. 7a), which is observed for many ophiolite-hosted chromitites from other supra-subduction zones. The Dehsheikh chromitites contain IPGE as well as Rh abundances between about 2 and 30 times the primitive mantle values and Pd abundances of about primitive mantle content. The PPGE/IPGE ratios

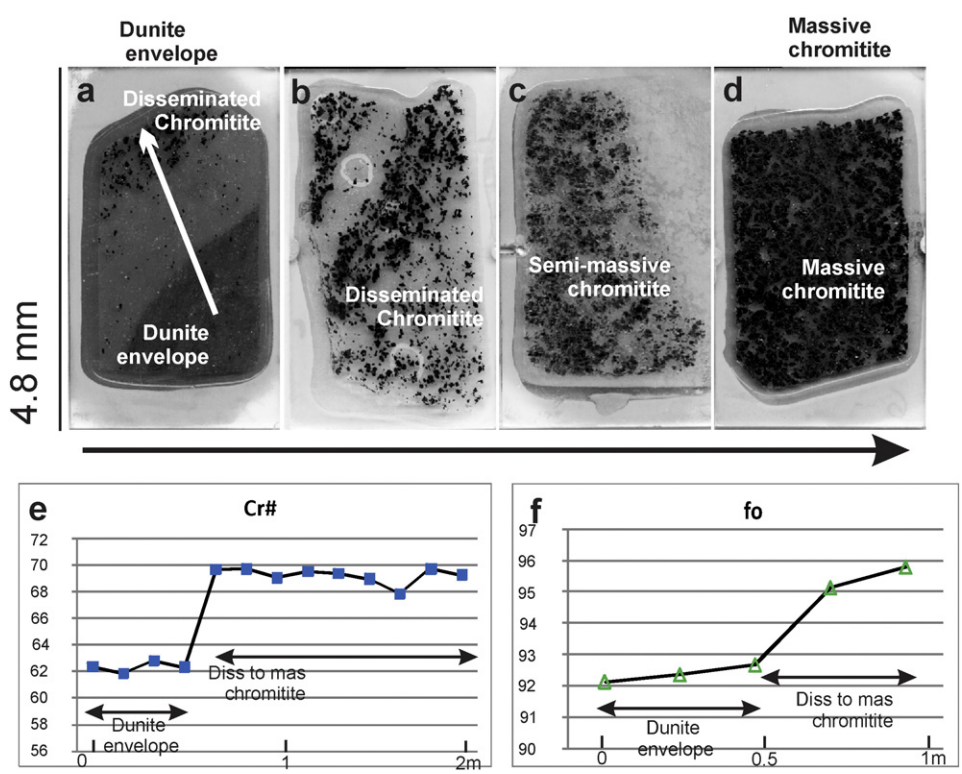

Fig. 4. a) Photographs of dunite envelope to disseminated and massive chromitites (a to d) and its compositional zoning for chromite (e) and olivine (f) Cr# and fo number.

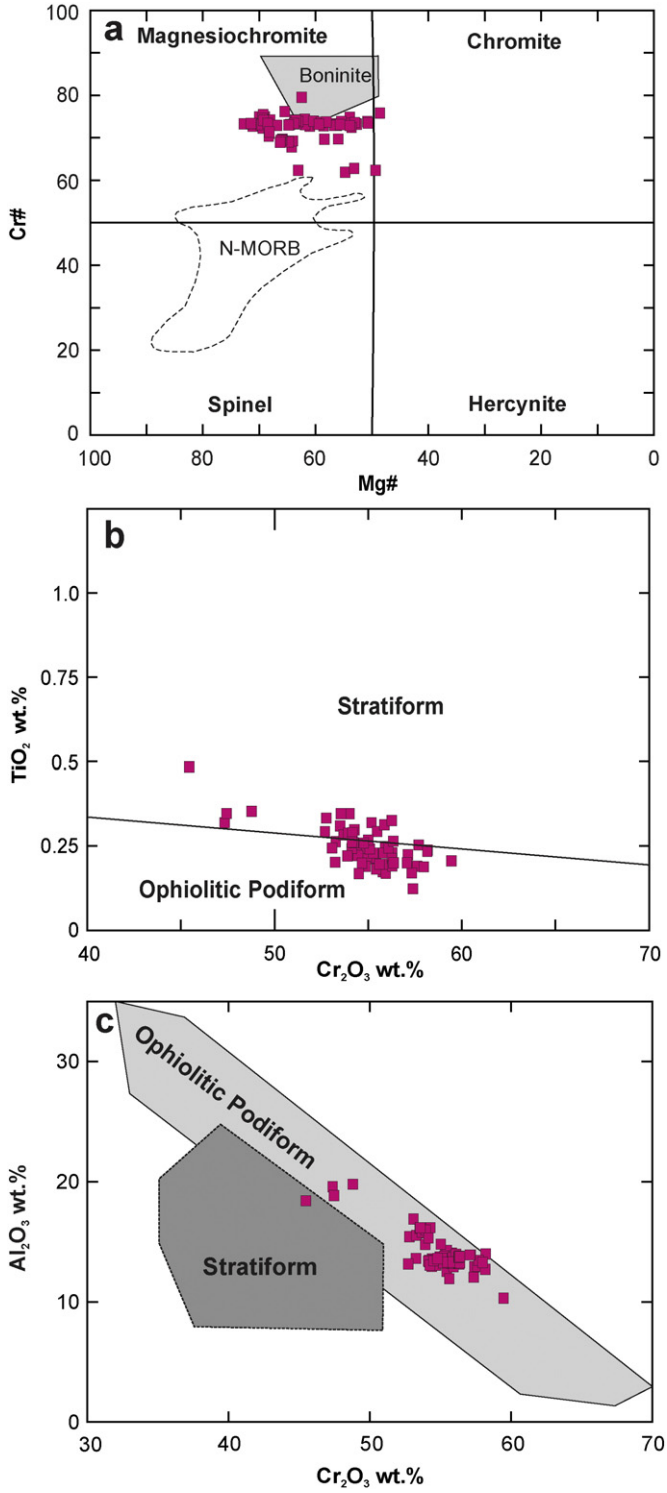

Fig. 5. a) Classification and compositional variation of chromian spinel from Dehsheikh chromitites in terms of Cr# [Cr/(Cr + Al)] versus Mg# [Mg/(Mg + Fe^{2+})] (fields for spinels in equilibrium with boninites and N-MORBs are after Dick and Bullen, 1984); b) TiO_2 versus Cr_2O_3 and c) Al_2O_3 vs. Cr_2O_3 diagrams showing the compositional variation of Dehsheikh chromitites. The stratiform and podiform chromitite fields are from Bonovia et al. (1993), and Ahmed and Arai (2003).

vary from 0.17 to 0.05, which are similar to other ophiolitic complexes (Fig. 7b), for example Troodos (Cyprus) and Semail ophiolites (Prichard et al., 2008), the Urals (Garuti et al., 2005; Melcher et al., 1997), Turkish ophiolites (Dönmez et al., 2014; Uysal et al. 2007a,b, 2009a,b) and Iranian ophiolites (Jannessary et al., 2012; Najafzadeh and Ahmadipour, 2014). However, higher ΣPGE contents and elevated concentrations of PPGE compared to IPGE were also found in ophiolitic mantle chromitites e.g., the Berit (Kozlu et al., 2014) and Muğla (Uysal et al., 2009a) ophiolites from Turkey, the Al'Ays ophiolitic complex (Prichard et al., 2008), the Shetland ophiolites (Prichard and Lord, 1994), Leka in Norway (Pedersen et al., 1993), the Thetford ophiolites (Corrivaux and Laflamme, 1990) and high Cr chromitites from the Sagua de Tanamo ophiolite in Cuba (González-Jiménez et al., 2011). The diagram of bulk PGE concentration vs. $PPGE_N/IPGE_N$ (Fig. 7b) was used to illustrate different PGE distribution patterns of chromitites. This expands an approach by Leblanc (1991) who used Pd/Ir as a fractionation factor. The Dehsheikh chromitites show a negative correlation and follow the ophiolitic trend that is in part similar to the trend of podiform chromitites from the Eskişehir ophiolite, NW-Turkey (Uysal et al., 2009b), and chromitites from the Kempirsai ophiolite massif, Urals (Melcher et al., 1999), but extends to lower total PGE concentrations.

7. Discussion

7.1. Parental melt composition of Dehsheikh podiform chromitites

The geochemical composition of chromium spinel provides valuable information on the petrogenesis of magmatic processes within different geodynamic environments (Augé, 1987; Barnes, 1986; Bedard, 1999; Dick and Bullen, 1984; Irvine, 1967; Kamenetsky et al., 2001; Melcher et al., 1997; Rollinson, 2008; Zhou et al., 1996). It is generally accepted that parental melts of chromitites can be generated by different processes, e.g., different degrees of partial melting (e.g., Arai, 1994; Irvine, 1977; Kelemen et al., 1992; Zhou et al., 1996), melt/rock reaction and melt/melt interactions in supra-subduction mantle sources (e.g., Kamenetsky et al. 2001; Melcher et al., 1999; Uysal et al., 2005, 2009a; Zhou et al., 1998). Several studies indicate that Al_2O_3 and TiO_2 concentrations and FeO/MgO ratios of chromites are directly related to the parental melt composition (Kamenetsky et al., 2001; Roeder and Reynolds, 1991; Rollinson, 2008).

In order to estimate melt compositions, we used the equations derived by Rollinson (2008) on the basis of chromite–melt inclusion data of Kamenetsky et al. (2001) to compute the Al and Ti concentrations of arc parental melt:

$$Al_2O_3-melt = 5.2181 \times Ln(Al_2O_3-chromite)–1.0505$$

$$Ln(TiO_2-melt) = 1.0963 \times (TiO_2-chromite)^{0.7863}.$$

The Al_2O_3 and TiO_2 concentrations of inferred parental melts of Dehsheikh chromitites vary from 11.1 to 14.5 wt.% and 0.21 to 0.49 wt.%, respectively (Table 1; Fig. 8).

The FeO/MgO ratios in the parental melt of the Dehsheikh chromitites were also calculated using the empirical formula cited in Augé (1987). This relationship is mostly applied to massive-texture chromitite with lesser amounts of intercumulus olivine. The FeO/MgO ratios were calculated to vary between 0.99 and 1.2.

$$\mathrm{Ln(FeO/MgO)_{chromite}} = 0.47–1.07 \times Y^{Al}{}_{chromite} + 0.64 \times Y^{Fe3+}{}_{chromite} + \mathrm{Ln(FeO/MgO)_{liquid}}$$

$$\text{where } Y^{Al}{}_{chromite} = Al/\left(Al + Cr + Fe^{3+}\right), Y^{Fe3+}{}_{chromite} = Fe^{3+}/\left(Al + Cr + Fe^{3+}\right)$$

In Fig. 9 the calculated concentrations of Al_2O_3 and TiO_2 in the melt are compared with those from Cape Vogel (Papua New Guinea) and Troodos boninites, boninites from other worldwide localities, MORB, and experimental melts of depleted mantle (DM). The chromitite samples from the Dehsheikh chromitites have relatively low TiO_2 and Al_2O_3

Table 2
Representative olivine chemical composition of Dehsheikh chromitites and their dunite envelope.

Sample	M5-1	M3-2	3	5	5	M1-2	M1-2	M1-2	M5-3	M5-3	F5	F5	F5
Texture	Nod	Mass	Diss	Mass			Band		Nod		Diss		
Chr/Ol	60%	80%	10%	80%			50%		60%		50%		
Mine	Godar	Emam Ali	Bozorgi				Avali		Godar		Avali		
SiO_2	41.49	41.89	41.35	41.54	41.35	41.49	41.71	41.25	41.54	41.18	41.54	41.44	41.73
TiO_2	0.00	0.02	0.04	0.01	0.04	0.00	0.02	0.01	0.00	0.02	0.009	0.00	0.051
Al_2O_3	0.01	0.01	0.01	0.04	0.00	0.00	0.00	0.01	0.01	0.02	0.00	0.00	0.00
Cr_2O_3	0.02	0.23	0.01	0.01	0.29	0.00	0.00	0.60	0.00	0.01	0.015	0.00	0.00
FeO	4.01	3.21	7.13	4.33	3.64	5.47	5.88	4.39	5.73	6.03	5.65	5.65	5.60
MnO	0.08	0.06	0.10	0.07	0.08	0.08	0.08	0.08	0.08	0.11	0.106	0.03	0.05
MgO	52.78	54.33	50.55	52.41	53.0	51.96	52.40	53.65	52.18	52.19	51.41	52.61	52.15
CaO	0.01	0.02	0.02	0.00	0.00	0.05	0.02	0.05	0.03	0.03	0.015	0.03	0.03
NiO	0.93	0.85	0.57	0.78	0.84	0.70	0.60	0.65	0.48	0.66	0.56	0.63	0.69
Na_2O	0.04	0.00	0.01	0.02	0.00	0.02	0.00	0.00	0.00	0.00	0.029	0.00	0.008
Total	99.37	100.61	99.80	99.22	99.27	99.78	100.71	100.70	100.04	100.26	99.33	100.42	100.32
Fo	95.82	96.71	92.55	95.50	96.21	94.28	93.97	95.47	94.1	93.77	94.1	94.25	94.23

Diss: disseminated, Mass: massive, Nod: nodular, Band: banded.

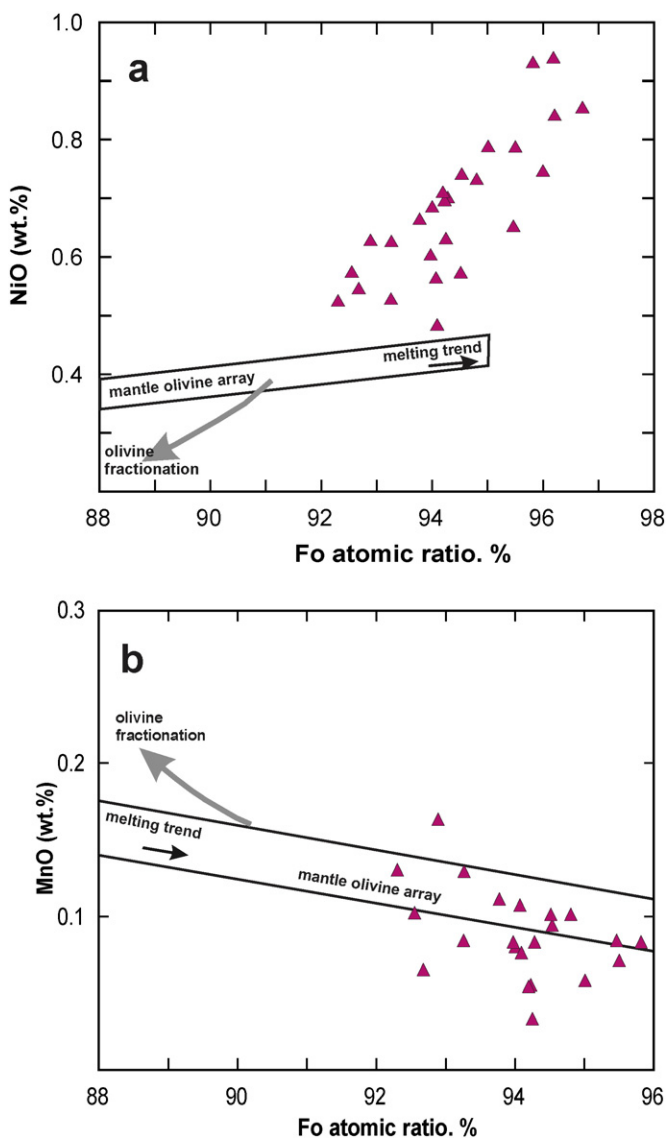

Fig. 6. a) NiO and b) MnO vs. Fo of olivine from dunite envelope to disseminated to massive chromitite from the Dehsheikh massif. Partial melting trends are from Ozawa (1994), and fractionation trends are from Ozawa (1994) and Nakamura (1995).

contents, and plot far from the MORB field, but show affinity with melts derived from depleted mantle, such as Troodos and Cape Vogel boninites. In Table 4 we provide additional parameters for comparison. The calculated parental melt FeO/MgO ratios of Dehsheikh chromitites are similar to boninite (Falloon et al., 2008) and some Turkish chromitite parental melts, but higher than those of the Soghan and Sorkhband chromitites (Esfandagheh–HajiAbad region). Al_2O_3 and TiO_2 of the inferred Dehsheikh melts show similarities to parental melts from chromitites in Oman (Rollinson, 2008), Turkey (Uysal et al., 2009a), eastern Cuba (Gonzáles-Jiménez et al. 2011), and Thailand (Orberger et al. 1995), which all seem to have affinities with boninitic melts.

7.2. Control on platinum-group-element distribution in the Dehsheikh chromitites

It is widely accepted that melting of mantle sulphides and alloys in peridotites provides the PGE content of magmas (e.g., Büchl et al., 2002; González-Jiménez et al., 2011; Lorand et al., 1999, Lorand et al., 2010; Prichard et al., 2008). Therefore, the melting regime can have a major impact on the PGE signature of the different basaltic magmas and, in turn, chromitites as their crystallization products. The existence of a critical melting stage releasing the PGE into the partial melt and occurring within a narrow interval of increasing melt generation has been suggested by Hamlyn and Keays (1986) and Prichard et al. (2008). It has been argued that approximately 20% to 25% melting of mantle is needed to remove all sulphide phases and extract PGE into the melts (e.g., Keays, 1995; Prichard et al., 2008). In different ophiolite settings, the average degree of partial melting varies from about 10% to 20% in mid-ocean ridge settings (Hofmann, 1988; Klein and Langmuir, 1987) to >20% in arc-related environments (Barnes and Prichard, 1993; Keays, 1995). In supra-subduction zones, moderate- to high-degree (≥20%) melts, such as boninites, cause sulphides in the mantle to be completely consumed and, in turn, IPGE to be enriched in the melts. As a result the chromitites having crystallized from boninites tend to have PGE contents of a hundred to thousands of ppb (e.g., Ahmed and Arai, 2002; Economou-Eliopoulos, 1996; Gervilla et al., 2005; González-Jiménez et al., 2011; Konstantopoulou and Economou-Eliopoulos, 1991; Prichard et al., 2008; Proenza et al., 1999; Uysal et al., 2009a; Zhou et al., 1998).

Basaltic melts at spreading centres, such as mid-ocean ridges or back-arc basins, form from degrees of melting ≤20%, i.e., small enough to leave sulphides behind in the residual mantle, thus producing low-PGE melts from which chromitites low in PGE will precipitate (no more than a few tens of ppb, e.g., Ahmed and Arai, 2002; Economou-Eliopoulos, 1996; Gervilla et al., 2005; Graham

Table 3
Whole rock PGE concentrations (ppb) in the Dehsheikh chromitites.

Sample	M1-2	M2-3	M3-2	M3-2-1	M4-1	M4	M4t	M5-1	M6	9
Texture	Band	Band	Nod	Band	Nod	Band	Mass	Nod	Diss	Mass
Chr. abundance	50%	60%	60%	50%	80%	50%	>90%	80–90%	70%	>90%
Mine name	Avali	Emam Ali	Emam Ali	Emam Ali	Abdashti	Abdashti	Abdashti	Godar	Godar	Bozorgi
Au	3	3	2	3	2	4	3	4	3	4
Ir	15	33	11	15	17	15	69	13	15	47
Os	12	35	8	14	11	13	54	10	11	79
Pd	4	2	2	4	3	4	2	4	2	5
Pt	b.d.l.	b.d.l.	b.d.l.	b.d.l.	1	2	b.d.l.	2	b.d.l.	5
Rh	4	9	6	6	8	5	13	5	5	9
Ru	42	77	35	41	43	44	142	40	38	161
Total	80	159	64	83	85	87	283	78	74	310

Detection limit is 1 ppb for PGEs and 2 ppb for Au. b.d.l. = below detection limit. Abbreviations are: Mass: massive; Diss: disseminated; Nod; nodular; Band: banded.

et al., 1996; Proenza et al., 1999; Uysal et al., 2007a, Uysal, 2008, 2009a; Zhou et al. 1998). The investigation of chromitites from the Al'Ays ophiolite complex led Prichard et al. (2008) to argue that PGE-enriched chromitites crystallized from melts generated within a critical melting interval at around 20%–25% of mantle melting.

During percolation through residual harzburgite the parental melts of chromitites will cause any remaining sulphide, which should be enriched in IPGE as the consequence of previous melt extraction, to dissolve in the melt (González-Jiménez et al., 2011; Marchesi et al., 2006, 2010; Uysal et al. 2015). Thus, continuous melt/rock reaction can control Cr#'s and PGE contents of chromitites and dunite envelopes. Therefore, it has been suggested that the boninitic parental melts of high Cr chromitites can become even more enriched in the PGE and Cr as a consequence of melt–rock interaction (González-Jiménez et al., 2011).

Partial melting of the mantle leads to the formation of either S-saturated or S-undersaturated melts. If S-saturated melt forms, it is initially low in PGE, because these elements will be mostly retained in residual sulphides. When a S-undersaturated magma is formed by high degrees of partial melting, no sulphide droplets will exsolve from this magma until sulphide saturation is achieved through fractional crystallization of silicate and oxide minerals; thus, the PGE will remain in the melt and become slightly more concentrated (Seitz and Keays, 1997). Experimental petrologic studies have indicated that MORB is S-saturated (Keays, 1995; Patten et al., 2013; Peach et al., 1990).

IPGE and PPGE have different solubilities in silicate magmas, the IPGE being more refractory and compatible for fractionating minerals than PPGE (Barnes et al., 1985). This contrasting geochemical behaviour is reflected by the Pd/Ir ratio, maybe considered as an 'index of fractionation' of the PGE during petrological processes. Pd/Ir is expected to increase in a melt undergoing fractional crystallization and reach ratios much higher than one in differentiated melts. It should be less than one in residual mantle material and decrease in melts generated at increasing degrees of partial melting of the mantle. The Pd/Ir ratios from the Dehsheikh chromitites are lower than one (0.02 to 0.3) and, therefore, much better match values inferred for the partial melting trend, being the most important process in chromitite formation.

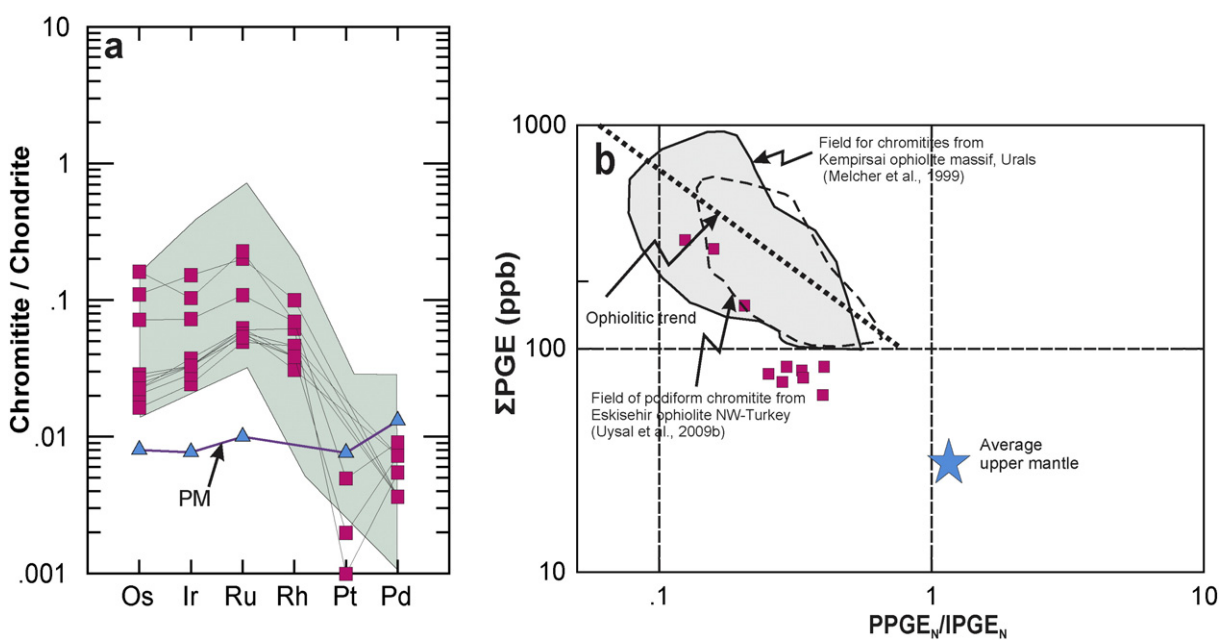

Fig. 7. a) CI-Chondrite-normalized (McDonough and Sun, 1995) PGE patterns of the Dehsheikh chromitites. Green field is for Cr-rich ophiolitic chromitite from supra-subduction zone settings. Data sources include: Economou-Eliopoulos (1996), Kocks et al. (2007), Uysal et al. (2007a, 2007b, 2009a, 2009b), Melcher et al. (1999), Garuti et al. (2005), Proenza et al. (1999), and Zhou et al. (1998). The normalized primitive mantle (PM) abundances from Becker et al. (2006) are given for comparison (blue triangles); b) PGE concentrations vs. chondrite-normalized PPGE/IPGE ratios for the Dehsheikh chromitites. Chondrite and average upper mantle values are from McDonough and Sun (1995) and Becker et al. (2006). Field for chromitites from the Kempirsai ophiolitic massif, Urals (Melcher et al., 1999) and field of podiform chromitite from Eskişehir ophiolite NW-Turkey (Uysal et al., 2009b) are shown for comparison. In cases where Pt was below the detection limit, we assumed an abundance of zero to calculate ∑PPGE. The error thus introduced is small and does not affect our reasoning.

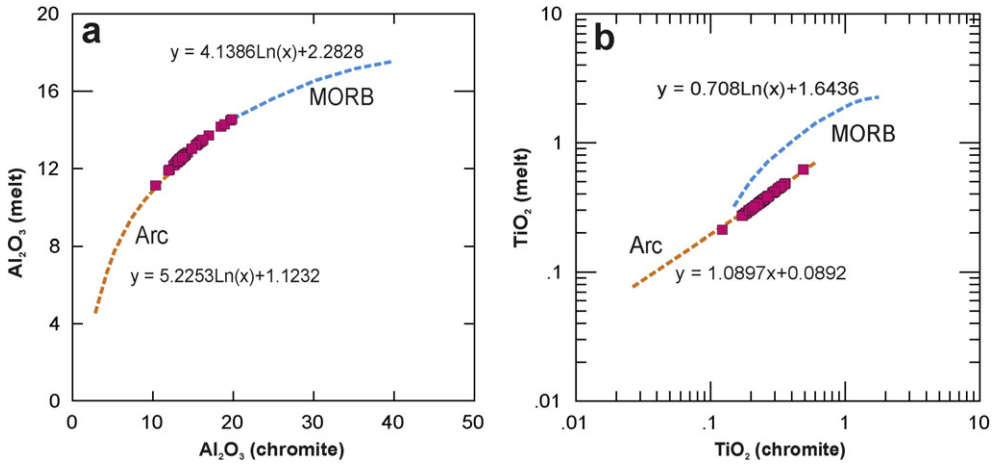

Fig. 8. a) Al_2O_3, b) TiO_2 contents of the melts in equilibrium with Dehsheikh chromitites. The MORB and Arc lines and regression equations are from Rollinson (2008).

The high IPGE/PPGE ratios of Dehsheikh chromitites (Fig. 7a) are more indicative of a melt derived from a mantle source that had already been depleted in PPGE by a prior stage of partial melting. Therefore, the bulk of the PPGE in the source were extracted into an early low- to intermediate-degree partial melt. Subsequently and possibly unrelated to this event, a second stage of higher degree partial melting of this PPGE-depleted source was responsible for the high IPGE/PPGE of these chromitites.

7.3. Genesis and geotectonic environment

The genesis of podiform chromitites is not well understood and several models have been proposed to account for their formation. Fractional crystallization from a continuously supplied melt circulating through magmatic conduits has been considered as the primary class of models (Lago et al. 1982; Leblanc and Ceuleneer, 1992; Thayer 1964). Other processes such as multi-stage partial melting, magma segregation, melt/rock reaction, and magma mixing within the upper mantle may also be involved during magma generation (Leblanc and Ceuleneer, 1992; Paktunc et al., 1990). Such models assume that melt/rock interaction and subsequently melt/melt mixing are the most important processes in the formation of podiform chromitites (Arai and Yurimoto, 1994; Kelemen, 1990; Zhou et al., 1996). Recently Gonzales-Jimenez et al. (2014) have proposed an integrated model where ophiolitic chromitites are commonly formed within networks of interconnected, high-porosity dunite channels, which had been generated by melt/rock reaction in mantle peridotites. Mixing and crystallization of new basaltic melts in these high-porosity and high-permeability channels provide an ideal setting for chromitite formation. The different textures, sizes, and types of the chromitites may reflect melt flow within this high porosity network of melt channels at different melt/rock ratios, and a range of temperature contrasts between melts and the host peridotites. In this model, hydro-fractures penetrating peridotites can promote chromitite formation from Cr-bearing fluids.

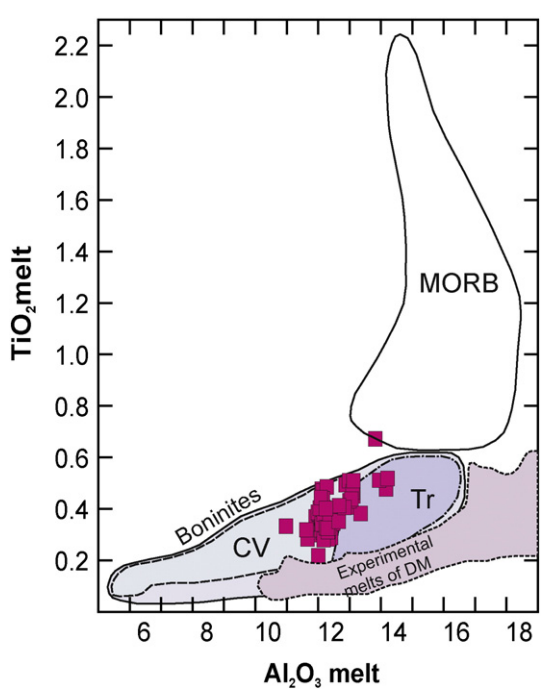

Fig. 9. TiO_2 and Al_2O_3 contents (wt.%) of melts in equilibrium with chromite from the Dehsheikh podiform chromitites. Boninite and MORB data were compiled from the literature and are shown for comparison. The CV (Cape Vogel) and Tr (Troodos) boninite, as well as MORB fields, are from Pagé and Barnes (2009) and references therein. Experimental melts of depleted mantle (DM) are from references in Rollinson (2008).

Morphological and structural features in the studied rocks, such as various textural layering, exhibition of sharp contacts between chromitites and their dunite envelope, dunite bands intercalated with chromitite layers, the lack of any obvious correlation between the size of chromitite pods, and the thickness of their dunite envelopes are all in favour of a model in which metasomatic–magmatic processes have taken place in a network of channels. Melt percolated through these channels and reacted with dunite.

The chemical composition of chromite is widely used as an indicator of magmatic formation that can provide clues on the tectonic setting (Dick and Bullen, 1984; Kamenetsky et al., 2001). The high Cr# of almost all chromitites can be related to boninitic magmas (Johnson et al., 1985). The high Cr# (68–79) and low TiO_2 contents (<0.3%) of the Dehsheikh chromitites are typical of Cr-rich chromitites (e.g., Zhou et al., 2001) formed in an arc setting (Arai et al., 2006). Chromite compositional variations such as TiO_2 vs. Cr# show a good match with variations in chromitites crystallized from boninitic melts, formed in supra-subduction zones (Fig. 10). In the TiO_2 vs. Al_2O_3 plot of Fig. 11, introduced by Zaccarini et al. (2011) to discriminate between spinels precipitated from MORB-, OIB-, and arc-related basaltic melts, the Dehsheikh chromitites display a broadly positive trend and fall within or close to the arc-type field, thus suggesting an island arc tholeiite to boninite affinity. In addition, computed Al_2O_3 and TiO_2 contents of parental melts are indicative of boninites, which are related to supra-subduction tectonic settings. The Cr# of chromite and Fo contents of olivine grains from the investigated transitional zone show

Table 4
Comparison between parental melt composition of Dehsheikh chromitites and other worldwide high Cr# podiform chromitites.

	Cr#	Al_2O_3-chromite	Al_2O_3-melt	TiO_2-chromite	TiO_2-melt	FeO/MgO-melt	Reference
Dehsheikh chromitites	0.68–0.79	10.2–16.1	11.1–14.5	0.12–0.27	0.21–0.49	0.99–1.2	This study
Soghan chromitites (Iran)	0.79–0.83	9.3	10.57	0.18	0.28	0.74	Najafzadeh et al., 2008
Sorkhband chromitites (Iran)		9.32	10.05	0.08		0.7	Najafzadeh and Ahmadipour, 2014
Shetland ophiolites	0.72	14.29	11.86–14.51	0.12			Brough et al., 2015
Sagua de Tanamo (eastern Cuba)	0.63–0.72	16.2	13.4	0.19	0.3	0.9–1.5	Gonzáles-Jiménez et al., 2011
Mugla ophiolite (Turkey)	0.64–0.75		8.8–10.5		0.23–0.34	0.3–1.1	Uysal et al., 2009a
Elekdag ophiolite (northern Turkey)	0.65–0.89	5.1–18.2	9.4–13.2	0.14–0.26	0.2–0.4	0.4–1.9	Dönmez et al., 2014
Oman ophiolite	0.71–0.77	11.7–14.4	11.8–12.9		0.23–0.34		Rollinson, 2008
Kempirsai (Kazakhstan)			9–10.6			0.3–0.5	Melcher et al., 1997
Santa Elena ultramafic nappe (Costa Rica)	0.81	10.3–17.5	11.2–13.0	0.14–0.2	0.28–0.38		Zaccarini et al., 2011
Nan Uttardite chromitites (Thailand)			11.6–12.0				Orberger et al., 1995
Boninite			11.29–14.87		0.24–0.22	0.68–0.89	Falloon et al., 2008
MORB			~14.70			~1.37	Gale et al., 2013

significant increases from dunite envelopes to disseminated and massive chromitites. Similar trends were reported by Zhou et al. (1996) and Xiong et al. (2015), and were interpreted as the result of melt/rock reaction between mantle peridotites and later boninitic melts formed in a supra-subduction zone.

The presence of amphibole inclusions in chromite grains provides indirect evidence that the examined chromitites crystallized from a Na-bearing hydrous melt. Boninite melts are known to be rich in water (Dobson et al., 1995) and are generally sulphide undersaturated (e.g., Keays, 1995). The very low PPGE concentrations of chromitites from the studied area might be the consequence of their earlier extraction into a low- to moderate-degree partial melts unrelated to boninitic melt formation. IPGE were partly extracted during the second, higher degree melting event that caused the boninitic melt to be S-undersaturated.

The combined lines of evidence presented above suggest that a boninitic melt played an important role in the formation of the Dehsheikh chromitites that intruded the mantle wedge above a subducted slab (e.g., Zhou et al., 1998). Such a geotectonic regime is considered to be the most likely one for the formation of boninites (e.g., Ahmed and Arai, 2002; Rollinson, 2008; Uysal et al., 2015).

According to Sahfaii Moghadam and Stern (2011) and Rajabzadeh et al. (2013), the Dehsheikh complex is part of the Esfandagheh–Haji Abad ophiolites that belong to the outer Zagros ophiolite belt. This belt represents autochthonous fore-arc lithosphere having formed by seafloor spreading along the southern margin of Eurasia. The chemical composition of chromites from Dehsheikh chromitites is indicative of crystallization from boninitic parental melts, which also has been already suggested for other Esfandagheh–Haji Abad ophiolitic complexes. Besides, the chemical composition of clinopyroxene from different lithologies at Dehsheikh complex, such as their higher Mg#, is indicative of a fore-arc setting (Fig. 8 in Peighambari et al., 2011). Thus, we envisage formation of the Dehsheikh complex in a fore-arc setting similar to that inferred for other outer Zagros ophiolites such as Soghan (Najafzadeh and Ahmadipour, 2014).

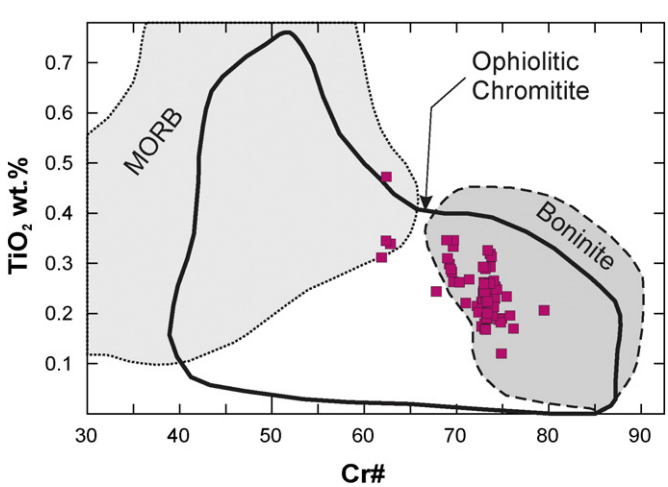

Fig. 10. TiO_2 vs. Cr# for chromites from Dehsheikh podiform chromitites. The podiform chromitite field is from Pagé and Barnes (2009) and references therein. Fields for chromite from MORB and boninite are from Barnes and Roeder (2001).

8. Conclusions

On the basis of field, petrographic, geochemical, and mineral compositional data on the Dehsheikh chromitites, the genesis of these chromitites is best explained by crystallization from melts ascending through networks of melt channels, formed by different degrees of melt–rock interaction. The high Cr#, low TiO_2, and relatively low PGE concentrations combined with high IPGE/PPGE ratios of these chromitites, as well as the presence of Na-bearing amphibole inclusions, are consistent with an origin of the parent liquids generated by high degrees of mantle partial melting that caused the melts to be S-undersaturated and hydrous. These inferred melts are boninitic in composition and may be linked to arc-related environments. Formation in a fore-arc setting appears as the most plausible scenario in this southeastern portion, but also in other parts of the outer Zagros ophiolites.

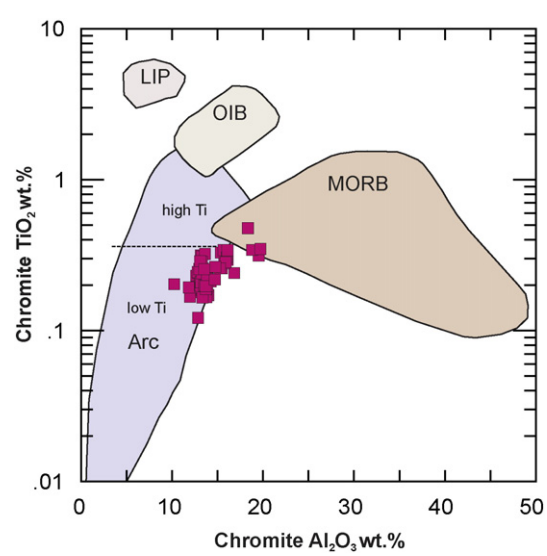

Fig. 11. TiO_2–Al_2O_3 variation of chromites from the Dehsheikh chromitites. The encircled fields are from Kamenetsky et al. (2001). LIP = large igneous province basalt, Arc = arc-related volcanic rocks. The Dehsheikh podiform chromitites plot close to, or within, the boninite field consistent with the interpretation that they formed from the boninitic melt associated with the Esfandagheh crust.

Acknowledgments

We are greatly indebted to Dr. Berndt (University of Münster) and Mr. Zibat (KIT) for their assistance with the electron microprobe analyses and SEM photographs, respectively. The authors acknowledge all other people who have supported us in this research. We are particularly grateful for the constructive comments of Maria Economou-Eliopoulos, Iain McDonald, Peter Lightfoot, and David Lentz that led to substantial improvements of the manuscript.

References

Najafzadeh, A.R., Ahmadipour, H., 2014. Using platinum-group elements and Au geochemistry to constrain the genesis of podiform chromitites and associated peridotites from the Soghan mafic–ultramafic complex, Kerman, southeastern Iran. Ore Geol. Rev. 60, 60–75.
Ahmadipour, H., Sabzehei, M., Whitechurch, H., Rastad, E., Emami, M.H., 2003. Soghan complex as an evidence for paleo spreading center and mantle diapirism in Sanandaj–Sirjan zone (south-east Iran). J. Sci. 14, 157–172.
Ahmed, A.H., 2013. Highly depleted harzburgite–dunite–chromitite complexes from the Neoproterozoic ophiolite, South Eastern desert, Egypt: a possible recycled upper mantle lithosphere. Precambrian Res. 233, 173–192.
Ahmed, A.H., Arai, S., 2002. Unexpectedly high PGE chromitite from the deeper mantle section of the northern Oman ophiolite and its tectonic implications. Contrib. Mineral. Petrol. 143, 263–278.
Ahmed, A.H., Arai, S., 2003. Platinum-group minerals in podiform chromitites of the Oman ophiolite. Can. Mineral. 41, 597–616.
Akmaz, R.M., Uysal, I., Saka, S., 2014. Compositional variations of chromite and solid inclusions in ophiolitic chromitites from the southeastern Turkey: implications for chromitite genesis. Ore Geol. Rev. 58, 208–224.
Arai, S., 1992. Chemistry of chromian spinel in volcanic rocks as a potential guide to magma chemistry. Mineral. Mag. 56, 173–184.
Arai, S., 1994. Compositional variation of olivine chromian spinel in Mg-rich magmas as a guide to their residual spinel peridotites. J. Volcanol. Geotherm. Res. 59, 279–294.
Arai, S., Yurimoto, H., 1994. Podiform chromitites of the Tari-Misaka ultramafic complex, southwest Japan, as mantle–melt interaction products. Econ. Geol. 89, 1279–1288.
Arai, S., Yurimoto, H., 1995. Possible subarc origin of podiform chromitites. Island Arc 4, 104–111.
Arai, S., Kadoshima, K., Morishita, T., 2006. Widespread arc-related melting in the mantle section of the northern Oman ophiolite as inferred from detrital chromian spinels. J. Geol. Soc. 163, 869–879.
Arai, S., Okamura, H., Kadoshima, K., Tanaka, C., Suzuki, K., Ishimaru, S., 2011. Chemical characteristics of chromian spinel in plutonic rocks: implication for deep magma processes and discrimination of tectonic setting. Island Arc 20, 125–137.
Augé, T., 1987. Chromite deposits in the northern Oman ophiolite: mineralogical constraints. Mineral. Deposita 22, 1–10.
Bacuta, G.C., Kay, R.W., Gibbs, A.K., Lipin, B.R., 1990. Platinum-group element abundance and distribution in chromite deposits of the Acoje block, Zambales ophiolite complex Philippines. J. Geochem. Explor. 37, 113–145.
Barnes, S.J., 1986. The effect of trapped liquid crystallization on cumulus mineral compositions in layered intrusions. Contrib. Mineral. Petrol. 93, 524–531.
Barnes, S.J., Pichard, C.P., 1993. The behaviour of platinum-group elements during partial melting, crystal fractionation and sulphide segregation: an example from the Cape Smith fold belt, northern Quebec. Geochim. Cosmochim. Acta 57, 79–87.
Barnes, S.J., Roeder, P.L., 2001. The range of spinel compositions in terrestrial mafic and ultramafic rocks. J. Petrol. 42, 2279–2302.
Barnes, S.J., Naldrett, A.J., Gorton, M., 1985. The origin of the fractionation of platinum-group elements in terrestrial magmas. Chem. Geol. 53, 303–323.
Becker, H., Horan, M.F., Walker, R.J., Gao, S., Lorand, J.-P., Rudnick, R.L., 2006. Highly siderophile element composition of the earth's primitive upper mantle: constraints from new data on peridotite massifs and xenoliths. Geochim. Cosmochim. Acta 70, 4528–4550.
Bedard, J.H., 1999. Petrogenesis of boninites from the Betts Cove ophiolite, newfoundland, Canada: identification of subducted source components. J. Petrol. 40, 1853–1889.
Bonavia, F.F., Diella, V., Ferrario, A., 1993. Precambrian podiform chromitites from Kenticha hill, southern Ethiopia. Econ. Geol. 88, 198–202.
Brough, C.P., Prichard, H.M., Neary, C.R., Fisher, P.C., McDonald, I., 2015. Geochemical variations within podiform chromitite deposits in the Shetland ophiolite: implications for petrogenesis and PGE concentration. Econ. Geol. 110, 187–208.
Büchl, A., Brügmann, G., Batanova, V.G., Münker, C., Hofmann, A.W., 2002. Melt percolation monitored by Os isotopes and HSE abundances: a case study from the mantle section of the Troodos ophiolite. Earth Planet. Sci. Lett. 204, 385–402.
Cai, K., Sun, M., Yuan, C., Zhao, G., Xiao, W., Long, X., 2012. Keketuohai mafic–ultramafic complex in the Chinese Altai, NW China: petrogenesis and geodynamic significance. Chem. Geol. 294–295, 26–41.
Corrivaux, L., Laflamme, J.H.G., 1990. Mineralogie des elements du groupe du platinedans les chromitites de l'ophiolite de Thetford mines, Quebec. Can. Mineral. 28, 579–595.
Dick, H.J.B., Bullen, T., 1984. Chromian spinel as a petrogentic indicator in abyssal and alpine-type peridotites and spatially associated lavas. Contrib. Mineral. Petrol. 86, 54–76.
Dobson, P.F., Skogby, H., Rossman, G.R., 1995. Water in boninite glass and coexisting orthopyroxene: concentration and partitioning. Contrib. Mineral. Petrol. 118, 414–419.
Dönmez, C., Keskin, S., Günay, K., Çolakoğlu, A.O., Çiftçi, Y., Uysal, İ., Türkel, A., Yıldırım, N., 2014. Chromite and PGE geochemistry of the Elekdağ ophiolite (Kastamonu, northern Turkey): implications for deep magmatic processes in a supra-subduction zone setting. Ore Geol. Rev. 57, 216–228.
Economou-Eliopoulos, M., 1996. Platinum-group element distribution in chromite ores from ophiolite complexes: implications for their exploration. Ore Geol. Rev. 11, 363–381.
Falloon, T.j., Danyushevsky, L.V., Crawford, A.J., Meffre, S., Woodhead, J.D., Bloomer, S.H., 2008. Boninites and adakites from the northern termination of the Tonga trench: implications for adakite petrogenesis. J. Petrol. 49, 697–715.
Gale, A., Dalton, A.D., Langmuir, C.H., Su, Y., Schilling, J.-G., 2013. The mean composition of ocean ridge basalts. Geochem. Geophys. Geosyst. 14, 489–518.
Garuti, G., Fershtater, G.B., Bea, F., Montero, P., Pushkarev, E., Zaccarini, F., 1997. Platinum-group elements as petrological indicators in mafic-ultramafic complexes of the central and southern Urals. Tectonophysics 276, 181–194.
Garuti, G., Pushkarev, E.V., Zaccarini, F., 2005. Diversity of chromite–PGE mineralization in ultramafic complexes of the Urals. In: Törmänen, T.O., Alapieti, T.T. (Eds.), Platinum Group Elements — from Genesis to Benefication and Environmental Impact. Oulu (Finland), August 8–11, 10th International Platinum Symposium, extended abstracts, pp. 341–344.
Gervilla, F., Proenza, J.A., Frei, R., González-Jiménez, J.M., Garrido, C.J., Melgarejo, J.C., Meibom, A., Díaz-Martínez, R., Lavaut, W., 2005. Distribution of platinum-group elements and Os isotopes in chromite ores from Mayarí–Baracoa ophiolite belt (eastern Cuba). Contrib. Mineral. Petrol. 150, 589–607.
Ghasemi, H., Juteau, T., Bellon, H., Sabzehei, M., Witechurch, H., Ricou, L.M., 2002. The mafic–ultramafic complex of Sikhoran (central Iran): a polygenetic ophiolitic complex. Geoscience 334, 431–438.
Ghosh, B., Morishita, T., Bhatia, K., 2013. Significance of chromium spinels from the mantle sequence of the Andaman Ophiolite, India: Paleogeodynamic implications. Lithos 164–167, 86–96.
González-Jiménez, J.M., Proneza, J.A., Gervilla, F., Melgarejo, J.C., Blanco-Moreno, J.A., Ruiz-Sanchez, R., Griffin, W.L., 2011. High-Cr and high-Al chromitites from the Sagua de Tánamo district, Mayarí–Cristal ophiolitic massif (eastern Cuba): constraints on their origin from mineralogy and geochemistry of chromian spinel and platinum-group elements. Lithos 125, 101–121.
González-Jiménez, J.M., Griffin, W.L., Proenza, J.A., Gervilla, F., O'Reilly, S.Y., Akbulut, M., Pearson, N.J., Arai, S., 2014. Chromitites in ophiolites: how, where, when, why? Part II. The crystallization of chromitites. Lithos 189, 140–158.
Graham, I.T., Franklin, B.J., Marshall, B., 1996. Chemistry and mineralogy of podiform chromitite deposits, southern NSW, Australia: a guide to their origin and evolution. Mineral. Petrol. 37, 129–150.
Hamlyn, P.R., Keays, R.R., 1986. Sulphur saturation and second stage melts; application to the Bushveld Pt metal deposits. Econ. Geol. 81, 1431–1445.
Hamlyn, P.R., Keays, R.R., Cameron, W.E., Crawford, A.J., Waldron, H.M., 1985. Precious metals in magnesian low-Ti lavas: implications for metallogenesis and sulphur saturation in primary magmas. Geochim. Cosmochim. Acta 49, 1797–1811.
Hofmann, A.W., 1988. Chemical differentiation of the earth: the relationship between mantle, continental crust, and oceanic crust. Earth Planet. Sci. Lett. 90, 297–314.
Irvine, T.N., 1967. Chromian spinel as a petrogenetic indicator. Part 2. Petrologic applications. Can. J. Earth Sci. 4, 71–103.
Irvine, T.N., 1977. Origin of chromitite in the Muskov intrusion and other stratiform intrusions: a new interpretation. Geology 5, 273–277.
Jannessary, M.R., Melcher, F., Lodziak, J., Meisel, T.C., 2012. Review of platinum-group element distribution and mineralogy in chromitite ores from southern Iran. Ore Geol. Rev. 48, 278–305.
Johnson, R.W., Jaques, A.L., Hickey, R.L., McKee, C.O., Chappell, B.W., 1985. Manam Island, Papua New Guinea: Petrology and geochemistry of a low-Ti basaltic island-arc volcano. J. Petrol. 26, 283–323.
Kamenetsky, V.S., Crawford, A.J., Meffre, S., 2001. Factors controlling chemistry of magmatic spinel: an empirical study of associated olivine, Cr-spinel and melt inclusions from primitive rocks. J. Petrol. 42, 655–671.
Keays, R.R., 1995. The role of komatiite and picritic magmatism and S-saturation in the formation of ore deposits. Lithos 34, 1–18.
Kelemen, P.B., 1990. Reaction between ultramafic wall rock and fractionating basaltic magma: part I, phase relations, the origin of calc-alkaline magma series, and the formation of discordant dunite. J. Petrol. 31, 51–98.
Kelemen, P.B., Dick, H.J.B., Quick, J.E., 1992. Formation of harzburgite by pervasive melt/rock interaction in the upper mantle. Nature 358, 635–641.
Klein, E.M., Langmuir, C.H., 1987. Global correlations of ocean ridge basalt chemistry with axial depth and crustal thickness. J. Geophys. Res. 92, 8089–8115.
Kocks, H., Melcher, F., Meisel, T., Burgath, K.P., 2007. Diverse contributing sources to chromitite petrogenesis in the Shebenik ophiolitic complex, Albania: evidence from new PGE- and Os-isotope data. Mineral. Petrol. 91, 139–170.
Konstantopoulou, G., Economou-Eliopoulos, M., 1991. Distribution of platinum-group elements and gold within the Vourinos chromitite ores, Greece. Econ. Geol. 86, 1672–1682.
Kozlu, H., Prichard, H., Melcher, F., Fisher, P., Brough, C., Stueben, D., 2014. Platinum group element (PGE) mineralisation and chromite geochemistry in the Berit ophiolite (Elbistan/Kahramanmaraş), SE Turkey. Ore Geol. Rev. 60, 97–111.
Lago, B., Rabinowicz, M., Nicolas, A., 1982. Podiform chromite ore bodies: a genetic model. J. Petrol. 23, 103–125.
Leblanc, M., 1991. Platinum-group elements and gold in ophiolitic complexes: distribution and fractionation from mantle to oceanic floor. In: Peters, T. (Ed.) Ophiolite Genesis and Evolution of the Oceanic Lithosphere, Oman. Kluwer, Dordrecht, pp. 231–260.
Leblanc, M., Ceuleneer, G., 1992. Chromite crystallization in a multicellular magma flow: evidence from a chromitite dike in the Oman ophiolite. Lithos 27, 231–257.

Lorand, J.-P., Alard, O., Luguet, A., 2010. Platinum-group element micronuggets and refertilization process in Lherz orogenic peridotite (northeastern Pyrenees, France). Earth Planet. Sci. Lett. 289, 298–310.
Lorand, J.P., Pattou, L., Gros, M., 1999. Fractionation of platinum-group elements and gold in the upper mantle: a detailed study in Pyrenean orogenic lherzolites. J. Petrol. 40, 957–981.
Marchesi, C., Garrido, C.J., Godard, M., Proenza, J.A., Gervilla, F., Blanco-Moreno, J., 2006. Petrogenesis of highly depleted peridotites and gabbroic rocks from the Mayarí–Baracoa ophiolitic belt (eastern Cuba). Contrib. Mineral. Petrol. 151, 717–736.
Marchesi, G., González-Jiménez, J.M., Gervilla, F., Garrido, C.J., Griffin, W.L., O'Reilly, S.Y., Proenza, J.A., Pearson, N.J., 2010. In situ Re–Os isotopic analysis of platinum-group minerals from the Mayarí–Cristal ophiolitic massif (Mayarí-Baracoa ophiolitic belt, eastern Cuba): implications for the origin of Os-isotope heterogeneities in podiform chromitites. Contrib. Mineral. Petrol. http://dx.doi.org/10.1007/S00410-010-0575-2.
McCall, G.J.H., 1997. The geotectonic history of the Makran and adjacent areas of southern Iran. J. Asian Earth Sci. 15, 517–531.
McDonough, W.F., Sun, S.S., 1995. The composition of the earth. Chem. Geol. 120, 223–253.
Melcher, F., Grum, W., Simon, G., Thalhammer, T.V., Stumpfl, E.F., 1997. Petrogenesis of the ophiolitic giant chromite deposits of Kempirsai, Kazakhstan: a study of solid and fluid inclusions in chromite. J. Petrol. 38, 1419–1458.
Melcher, F., Grun, W., Thalhammer, T.V., Thalhammer, O.A.R., 1999. The giant chromite deposits at Kempirsai, Urals: constrains from trace elements (PGE, REE) and isotope data. Mineral. Deposita 34, 250–272.
Najafzadeh, A.R., Arvin, M., Pan, Y., Ahmadipour, H., 2008. Podiform chromitites in the Sorkhband ultramafic complex, southern Iran: evidence for ophiolitic chromitite. J. Sci. 19, 49–65.
Nakamura, M., 1995. Residence time and crystallization history of nickeliferous olivine phenocrysts from the northern Yatsugatake volcanoes, central Japan: application of a growth and diffusion model in the system Mg–Fe–Ni. J. Volcanol. Geotherm. Res. 66, 81–100.
Naldrett, A.J., 1981. Platinum-group element deposits. Can. Inst. Min. Metall. Petrol. 23, 197–232.
Nicolas, A., 1989. Structure of Ophiolites and Dynamics of Oceanic Lithosphere. 367. Kluwer, Dordrecht.
Orberger, B., Lorand, J.P., Girardeau, J., Mercier, J.C.C., Pitragool, S., 1995. Petrogenesis of ultramafic rocks and associated chromitites in the Nan Uttaradit ophiolite, northern Thailand. Lithos 35, 153–182.
Ozawa, K., 1994. Melting and melt segregation in the mantle wedge above a subduction zone: evidence from the chromite-bearing peridotites of the Miyamori ophiolite complex, northeastern Japan. J. Petrol. 35, 647–678.
Pagé, P., Barnes, S.J., 2009. Using trace elements in chromites to constrain the origin of podiform chromitites in the Thetford Mines ophiolite, Québec, Canada. Econ. Geogr. 104, 997–1018.
Paktunc, A.D., Hulbert, L.J., Harris, D.C., 1990. Partitioning of the platinum-group and other trace elements in sulfides from the Bushveld complex and Canadian occurrences of nickel–copper sulfides. Can. Mineral. 28, 475–488.
Patten, C., Barnes, S.J., Mathez, E.A., Jenner, F.E., 2013. Partition coefficients of chalcophile elements between sulfide and silicate melts and the early crystallization history of sulfide liquid: LA-ICP-MS analysis of MORB sulfide droplets. Chem. Geol. 358, 176–188.
Peach, C.L., Mathez, E.A., Keays, R.R., 1990. Sulfide melt–silicate melt distribution coefficients for the noble metals and other chalcophile metals as deduced from MORB: implications for partial melting. Geochim. Cosmochim. Acta 54, 3379–3389.
Pedersen, R.B., Hohannesen, G.M., Boyd, R., 1993. Stratiform PGE mineralizations in the ultramafic cumulates of the Leka ophiolite complex central Norway. Econ. Geol. 88, 782–803.
Peighambari, S., Ahmadipour, H., Stosch, H.G., Daliran, F., 2011. Evidence for multi-stage mantle metasomatism at the Dehsheikh peridotite massif and chromite deposits of the Orzuieh coloured mélange belt, southeastern Iran. Ore Geol. Rev. 39, 245–264.
Prichard, H., Brough, C., 2009. Potential of ophiolite complexes to host PGE deposits. In: Li, Chusi, Ripley, Edward M. (Eds.), New Developments in Magmatic Ni-Cu and PGE Deposits. Geological Publishing House, Beijing, pp. 277–290.
Prichard, H.M., Lord, R.A., 1994. Evidence for differential mobility of platinum-group elements in the secondary environment in Shetland ophiolite complex. Trans. Inst. Min. Metall., Sect. B 103, 79–86.
Prichard, H., Neary, C.R., Potts, P.J., 1986. Platinum-group minerals in the Shetland ophiolite complex. In: Gallagher, M.J., Ixer, R.A., Neary, C.R., Prichard, H. (Eds.), Metallogenesis of Basic and Ultrabasic Rocks: Institute of Mining and Metallurgy Symposium Volume, Edinburgh, pp. 271–294.
Prichard, H.M., Neary, C.R., Fisher, P.C., O'Hara, M.J., 2008. PGE-rich podiform chromitites in the Al 'Ays ophiolite complex, Saudi Arabia: an example of critical mantle melting to extract and concentrate PGE. Econ. Geol. 103, 1507–1529.
Proenza, J.A., Gervilla, F., Melgarejo, J.C., Bodinier, J.L., 1999. Al and Cr rich chromitites from the Mayari–Baracoa ophiolitic belt, (eastern Cuba): consequence of interaction between volatile-rich melts and peridotite in suprasubduction mantle. Econ. Geol. 94, 547–566.
Rajabzadeh, M.A., Nazari Dehkordi, T., Caran, Ş., 2013. Mineralogy, geochemistry and geotectonic significance of mantle peridotites with high-Cr chromitites in the Neyriz ophiolite from the outer Zagros ophiolite belts, Iran. J. Afr. Earth Sci. 78, 1–15.
Roberts, S., 1988. Ophiolitic chromitite formation: a marginal basin phenomenon? Econ. Geol. 83, 1034–1036.
Roeder, P.L., Reynolds, I., 1991. Crystallization of chromite and chromium solubility in basaltic melts. J. Petrol. 32, 909–934.
Rollinson, P., 2008. The geochemistry of mantle chromitites from the northern part of the Oman ophiolite: inferred parental melt compositions. Contrib. Mineral. Petrol. 156, 273–288.
Sabzehei, M., 1974. Les Mélange Ophiolitiques de la Region dEsfandaghéh (Iran Meridonal)-Etude Petrologique et Structure, Interpretations Dans le Carde Iranian (Thesis) Université scientifiqueet Médicale de Grenoble, France.
Seitz, H.M., Keays, R.R., 1997. Platinum group element segregation and mineralisation in a noritic ring complex formed from Proterozoic siliceous high magnesium basalt magmas in the Vestfold hills, Antarctica. J. Pet. 38, 703–725.
Shafaii Moghadam, H., Stern, R.J., 2011. Geodynamic evolution of upper Cretaceous Zagros ophiolites: formation of oceanic lithosphere above a nascent subduction zone. Geol. Mag. 148, 762–801.
Shafaii Moghadam, H., Stern, R.J., Rahgoshay, M., 2010. The Dehshir ophiolite (central Iran): geochemical constraints on the origin and evolution of the inner Zagros ophiolite belt. Geol. Soc. Am. Bull. 122, 1516–1547.
Shafaii Moghadam, H., Mosaddegh, H., Santosh, M., 2013. Geochemistry and petrogenesis of the late Cretaceous Haji-Abad ophiolite (outer Zagros ophiolite belt, Iran): implications for geodynamics of the Bitlis–Zagros suture zone. Geol. J. 48, 579–602.
Shahabpour, J., 2005. Tectonic evolution of the orogenic belt in the region located between Kerman and neyriz. J. Asian Earth Sci. 24, 405–417.
Thayer, P.T., 1964. Principal features and origin of podiform chromite deposits, and some observations on the Guleman-Soridag district, Turkey. Econ. Geol. 59, 1497–1524.
Uysal, I., 2008. Platinum-group minerals (PGM) and other solid inclusions in the Elbistan-Kahramanmaras mantle-hosted ophiolitic chromitites, southeastern Turkey: their petrogenetic significance. Turk. J. Earth Sci. 17, 729–740.
Uysal, I., Sadiklar, M.B., Tarkian, M., Karsli, O., Aydin, F., 2005. Mineralogy and composition of the chromitites and their platinum-group minerals from Ortaca (Mugla-SW Turkey): evidence for ophiolitic chromitite genesis. Mineral. Petrol. 83, 219–242.
Uysal, I., Tarkian, M., Sadiklar, M.B., Sen, C., 2007a. Platinum-group elements geochemistry and mineralogy in ophiolitic chromitites from the Kop mountains, northeastern Turkey. Can. Mineral. 45, 355–377.
Uysal, I., Zaccarini, F., Garuti, G., Meisel, T., Tarkian, M., Bernhardt, H.J., Sadiklar, M.B., 2007b. Ophiolitic chromitites from the Kahramanmaraş area, southeastern Turkey: their platinum-group elements (PGE) geochemistry, mineralogy and Os-isotope signature. Ofioliti 32, 151–161.
Uysal, I., Tarkian, M., Sadiklar, M.B., Zaccarini, F., Meisel, T., Garuti, G., Heidrich, S., 2009a. Petrology of high-Cr and high-Al ophiolitic chromitites from the Muğla, SW Turkey: implications from composition of chromite, solid inclusions of platinum-group minerals, silicate, and base metal mineral, and Os-isotope geochemistry. Contrib. Mineral. Petrol. 158, 659–674.
Uysal, I., Zaccarini, F., Sadiklar, M.B., Tarkian, M., Thalhammer, O.A.R., Garuti, G., 2009b. The podiform chromitites in the Dagkuplu and Kavak mines, Eskisehir ophiolite (NW-Turkey): genetic implications of mineralogical and geochemical data. Geol. Acta 7, 351–362.
Uysal, I., Akmaz, R.M., Kapsiotis, A., Demir, Y., Saka, S., Avci, E., Muller, D., 2015. Genesis and geodynamic significance of chromitites from the Orhaneli and Harmancık ophiolites (Bursa, NW Turkey) as evidenced by mineralogical and compositional data. Ore Geol. Rev. 65, 26–41.
Xiong, F., Yang, J., Robinson, P.T., Dilek, Y., Milushi, I., Xu, X., Chen, Y., Zhou, W., Zhang, Z., Lai, S., Tian, Y., Huang, Z., 2015. Petrology and geochemistry of high Cr# podiform chromitites of Bulqiza, eastern Mirdita ophiolite (EMO), Albania. Ore Geol. Rev. 70, 188–207.
Zaccarini, F., Garuti, G., Proenza, J.A., Campos, L., Thalhammer, O.A.R., Aiglsperger, T., Lewis, J., 2011. Chromite and platinum-group-elements mineralization in the Santa Elena ophiolitic ultramafic nappe (Costa Rica): geodynamic implications. Geol. Acta 9, 407–423.
Zhou, M.F., Robinson, P.T., 1997. Origin and tectonic setting of podiform chromite deposits. Econ. Geol. 92, 259–262.
Zhou, M.F., Robinson, P., Malpas, J., Li, Z., 1996. Podiform chromites in the Luobusa ophiolite (southern Tibet): implications for melt rock interaction and chromite segregation in the upper mantle. J. Petrol. 37, 3–21.
Zhou, M.F., Keays, R.R., Kerrich, R.W., 1998. Controls on platinum-group elemental distributions of podiform chromitites: a case study of high-Cr and high-Al chromitites from Chinese orogenic belt. Geochim. Cosmochim. Acta 62, 677–688.
Zhou, M.F., Robinson, P.T., Malpas, J., Aitchison, J., Sun, M., Bai, J.W., Hu, X.F., Yang, S.J., 2001. Melt/mantle interaction and melt evolution in the Sartohay high Al chromite deposits of the Dalabute ophiolite (NW China). J. Asian Earth Sci. 19, 517–534.